Talc under tension and compression: Spinodal instability, elasticity, and structure

Lars Stixrude

Department of Geological Sciences, University of Michigan, Ann Arbor, Michigan, USA

Received 30 November 2001; revised 27 April 2002; accepted 9 May 2002; published 6 December 2002.

[1] Talc occurs as a product of alteration of ultramafic rocks and may be a significant constituent of oceanic lithosphere and the arc mantle wedge. We explore the physical properties and structure of talc over a wide pressure range with density functional theory using the variable cell shape plane wave pseudopotential method in the local density (LDA) and generalized gradient (GGA) approximations. For LDA, the theoretical equation of state agrees with room temperature experimental measurements of the volume to within 2% when estimated effects of lattice vibrations are accounted for. We predict a spinodal mechanical instability (vanishing bulk modulus) at a volume 4% larger than the experimental volume at ambient conditions. Results for compression and tension are well 2represented by a fourth-order Birch-Murnaghan finite strain expansion with K_0 = 37.8, $K_0' = 13.\ 6$, $K_0K_0'' = -153$, where K is the bulk modulus, primes indicate pressure derivatives and subscript 0 refers to zero pressure. The estimated theoretical value of K_0 at 300 K (29 GPa) is considerably less than that determined from the experimental equation of state, a difference we attribute to the constraints of strain compatibility in the polycrystalline laboratory sample. The $c^* = c \sin \beta$ axis is found to be a factor of 7 more compressible than the b axis, consistent with experimental data. Compression in the $a-b$ plane is accommodated primarily by the Mg-octahedra. The polyhedral bulk modulus of the Mg-octahedra is considerably greater than one-third the linear modulus of the a axis. The difference is attributed to the increasing regularity of the Mg-octahedra on compression as measured by the octahedral tilt angle. The t sheet maintains registry with the o sheet by rotation of the Si-tetrahedra; the tetrahedral rotation angle rises from a value of 3° at the experimental volume to a theoretically predicted value of 22° at a volume of 170 Å^3 where the pressure is 26 GPa. Tetrahedral rotation leads to small Si-O-Si angles at the highest pressures investigated (<122° at 26 GPa), which leads us to speculate that talc may undergo pressure-induced amorphization under low-temperature compression. *INDEX TERMS:* 1025 Geochemistry: Composition of the mantle; 3620 Mineralogy and Petrology: Crystal chemistry; 3919 Mineral Physics: Equations of state; 3924 Mineral Physics: High-pressure behavior; *KEYWORDS:* talc, crystal structure, compression mechanisms, first principles theory

Citation: Stixrude, L., Talc under tension and compression: Spinodal instability, elasticity, and structure, *J. Geophys. Res.*, *107*(B12), 2327, doi:10.1029/2001JB001684, 2002.

1. Introduction

[2] Talc $Mg_3Si_4O_{10}(OH)_2$ occurs most frequently as a product of metamorphism or hydrothermal alteration of ultramafic rocks [*Evans and Guggenheim*, 1988]. Observation of axial outcrops of peridotite [*Cannat*, 1993], and evidence for deep hydration (to several km) of ultramafic rocks [*Trommsdorff et al.*, 1998], suggest talc as an important phase in the oceanic crust. Talc may play a significant role in the transport of water to the mantle in subduction zones. Subducted metasediments are expected to transform to a talc-bearing assemblage that is stable from 2–5 GPa (60–150 km depth) [*Mysen et al.*, 1998]. Talc may also occur as the result of fluid release and metasomatism in the mantle wedge [*Bailey and Holloway*, 2000]. On its own composition, talc is stable to 5 GPa, where it transforms to an assemblage containing the 10 Å phase, a dense hydrous magnesium silicate with a structure closely related to that of talc [*Chinnery et al.*, 1999; *Fumagalli et al.*, 2001].

[3] Despite the important role that talc is likely to play in subduction zone processes, little is known of its properties at high pressure. A better understanding of the structure and thermodynamic properties of talc are important for further constraining the metamorphic reactions that form and consume this phase. Knowledge of the elasticity of talc will be important for interpreting seismological observations of subduction zones and detecting the presence of talc in this and other geologic settings. The crystal

0148-0227/02/2001JB001684$09.00

structure has been refined at ambient conditions [*Perdikatsis and Burzlaff*, 1981]. There has been one polycrystalline X-ray diffraction study in the diamond anvil cell at ambient temperature in which the lattice parameters were measured up to 10 GPa and the bulk modulus was derived by fitting to the equation of state [*Pawley et al.*, 1995]. The longitudinal wave velocity of talc has been measured at 0.5 GPa as a function of temperature [*Bailey and Holloway*, 2000]. Bailey and Holloway combined their measurements with the bulk modulus derived from the equation of state to calculate the shear wave velocity and Poisson ratio of talc.

[4] Talc is significant as a model hydrous phase for the shallower portions of the Earth's upper mantle. The structure of two other hydrous phases that are important in the subduction environment, chlorite and the 10 Å phase, also contain 2:1 magnesium silicate layers. All of these structures are relatively open as compared with nominally anhydrous upper mantle magnesium silicates such as forsterite. There has been considerable crystal chemical interest in establishing the ultimate limits of metastability of open structures, such as ice, quartz, and muscovite at high pressure [*Faust and Knittle*, 1994; *Hemley et al.*, 1988; *Mishima et al.*, 1984; *Richet and Gillet*, 1997]. In order to gain additional insight into compression mechanisms, we have extended our study of talc to pressures well beyond its thermodynamic stability limit, up to a pressure of 30 GPa. We also explore negative pressures and establish the limit of mechanical stability of talc under hydrostatic tension. In the limit of large tension, we find that talc dissociates into isolated 2:1 layers, the structure of which may be relevant for understanding the physics and chemistry of clay surfaces or of very small crystals of talc, for example, growth nuclei in solution.

[5] Density functional theory has proven to be a powerful tool for studying the structure and thermodynamic properties of Earth materials at high pressure [*Stixrude et al.*, 1998]. Within the plane wave pseudopotential method, the forces acting on the nuclei, and stresses acting on the lattice may be calculated, which permits symmetry-preserving structural relaxation and the prediction of the details of crystal structure at high pressure [*Wentzcovitch et al.*, 1993]. Talc, triclinic with 36 structural degrees of freedom, is one of the most complex Earth materials studied with first principles methods. There has been one previous first principles study of talc, but the experimental structure was assumed, and no structural relaxation was attempted [*Bridgeman et al.*, 1996]. The first principles methods used here are described in more detail below. A description of the results includes the predicted equation of state, lattice parameters, and internal structural parameters. These yield insight into the nature of mechanical instability in this phase, its elasticity, and how this is related to changes in the structure at high pressure.

2. Theory

[6] Our results are based on density functional theory [*Hohenberg and Kohn*, 1964; *Kohn and Sham*, 1965]. While the theory is exact, the exact form of the exchange-correlation functional is unknown and must be approximated. We investigate two widely used approximations: the local density approximation (LDA), and the more recently developed generalized gradient approximation (GGA) [*Lundqvist and March*, 1987; *Perdew et al.*, 1996]. In order to make the solution tractable, one other essential approximation is made: the pseudopotential approximation [*Heine*, 1970]. This approximation is physically motivated by the argument that the core electrons participate little in bonding and structural change over the range of interest. The nucleus and core electrons are replaced by a simpler object, the pseudopotential, which has the same scattering properties. We use ultra-soft Vanderbilt [*Vanderbilt*, 1990; *Kresse et al.*, 1992] pseudopotentials which limits the size of the plane wave basis set that is required to accurately represent charge density and potential.

[7] Computations are performed with the Vienna ab initio simulation package (VASP) [*Kresse and Hafner*, 1993; *Kresse and Furthmüller*, 1996a; *Kresse and Furthmüller*, 1996b]. Calculated forces and stresses are used to perform complete structural relaxations at constant volume. A conjugate gradient scheme systematically modifies the structure until net forces and deviatoric stresses fall below a tolerance threshold. The relaxation scheme is based on the method of *Wentzcovitch* [1991] and *Wentzcovitch et al.* [1993] which conserves the space group symmetry.

[8] We have assumed the triclinic $C\bar{1}$ space group, corresponding to the 1Tc polytype, as found in single crystal X-ray diffraction [*Perdikatsis and Burzlaff*, 1981] and all previous detailed structural analyses of talc [*Evans and Guggenheim*, 1988]. A high pressure polycrystalline X-ray diffraction study assumed a monoclinic unit cell with a doubled c axis, corresponding the 2M polytype [*Pawley et al.*, 1995]. The reason for the discrepancy between the symmetry assumed by Pawley et al. and other studies is unclear. All computations are performed in the primitive unit cell (21 atoms, i.e., one formula unit). Use of the primitive, rather than conventional, unit cell is important because the size of the unit cell is a primary determinant of computational cost. In order to facilitate comparison with experimental data, we express the lattice parameters (though not the volume) in terms of the conventional c-centered cell. We used an energy cutoff, E_{cut} = 600 eV, and a Monkhorst-Pack [*Monkhurst and Pack*, 1976] 2 × 2 × 2 k point mesh, yielding 4 k points in the irreducible wedge of the Brillouin zone. A series of convergence tests demonstrated that these computational parameters yield pressures that are converged to within 0.1 GPa. The Pulay stress [*Payne et al.*, 1992] was found to be 0.03 GPa.

[9] We analyze compressional and tensional behavior with two commonly used forms of the equation of state. In the Birch-Murnaghan formulation [*Birch*, 1978], the normalized pressure

$$F = \frac{P}{3f(1+2f)^{5/2}} \tag{1}$$

is expressed as a polynomial in the Eulerian volume finite strain

$$f = \frac{1}{2}\left[\left(\frac{V}{V_0}\right)^{-2/3} - 1\right], \tag{2}$$

where P is pressure and V is volume. In the case of the universal equation of state [*Vinet et al.*, 1987], the normalized pressure is

$$H = \frac{PX^2}{3(1-X)}. \quad (3)$$

The logarithm of H is a linear function of the linear compression

$$X = \left(\frac{V}{V_0}\right)^{1/3}. \quad (4)$$

The coefficients of the expansions may be related to the bulk modulus and its pressure derivatives.

[10] In order to analyze the compression of talc, we consider the anisotropic generalization of the bulk modulus and the equation of state. The compressibility is a symmetric tensor [*Nye*, 1985]

$$k_{ij} = \left(\frac{\partial \epsilon_{ij}}{\partial P}\right)_T, \quad (5)$$

where ϵ_{ij} are the elements of the strain tensor and the usual (volume) bulk modulus is related to the trace $K_0^{-1} = k_{11} + k_{22} + k_{33}$. For triclinic structures, all elements of the compressibility tensor are nonzero. For monoclinic structures, four of the off-diagonal elements are zero. The diagonal elements are the linear bulk moduli of the three orthogonal pseudoaxes

$$k_x = K_x^{-1} = \frac{1}{x}\left(\frac{\partial x}{\partial P}\right)_T, \quad (6)$$

where the axes, x, are a, b, and $c^* = c \sin \beta$. The nonzero off-diagonal element

$$k_{13} = \frac{1}{2}\sin\beta\left(\frac{\partial \beta}{\partial P}\right)_T, \quad (7)$$

where β is the angle between a and c axes. We find that the compression of talc is quasi-monoclinic over the pressure range of interest.

[11] Our results are for the static lattice; that is, the effects of lattice vibrations are ignored. In order to compare more directly our theoretical equation of state to that experimentally measured at room temperature, we have accounted approximately for vibrational terms via the Mie-Grüneisen relation [*Anderson*, 1995; *Ita and Stixrude*, 1992]

$$P(V,T) = P_{\text{static}}(V) + \frac{\gamma}{V}\left[E_{zp}(V) + E_{th}(V,T)\right] \quad (8)$$

$$K(V,T) = K_{\text{static}}(V) + \frac{\gamma}{V}(\gamma + 1 - q)\left[E_{zp}(V) + E_{th}(V,T)\right] - \frac{\gamma^2}{V} \cdot [TC_V(V,T)], \quad (9)$$

where P_{static} and K_{static} are the static values calculated from density functional theory, V is the volume, γ and q are the Grüneisen parameter and its logarithmic volume derivative, respectively, E_{zp} is the zero-point energy, E_{th} is the thermal energy, and C_V is the isochoric heat capacity. The zero-point energy depends on $\theta(1) = hc\nu(1)/k = 830$ K, where $\nu(1)$ is the mean frequency (first moment) of the vibrational density of states as calculated from the model of *Kieffer* [1980], h is the Planck constant, and c is the speed of light [*Barron and White*, 1999]. The thermal energy, E_{th} is calculated using the Debye model and depends on an assumed Debye temperature, θ_D. The Debye temperature is known to vary with temperature in talc [*Kieffer*, 1980]. Because our results do not depend strongly on the value of θ_D, we assume $\theta_D \approx \theta(1)$, an approximation that is tested below. The value for the Grüneisen parameter

$$\gamma = \frac{V\alpha K_T}{C_V} \quad (10)$$

is taken from experimental data [*Ahrens*, 1995]; we further assume that $q = 1$. Our approach to vibrational corrections has been used previously in a theoretical study of silica [*Stixrude and Bukowinski*, 1988] and differs from theoretical studies of close-packed materials in which vibrational parameters may be estimated solely on the basis of the static equation of state [*Aidun and Bukowinski*, 1984].

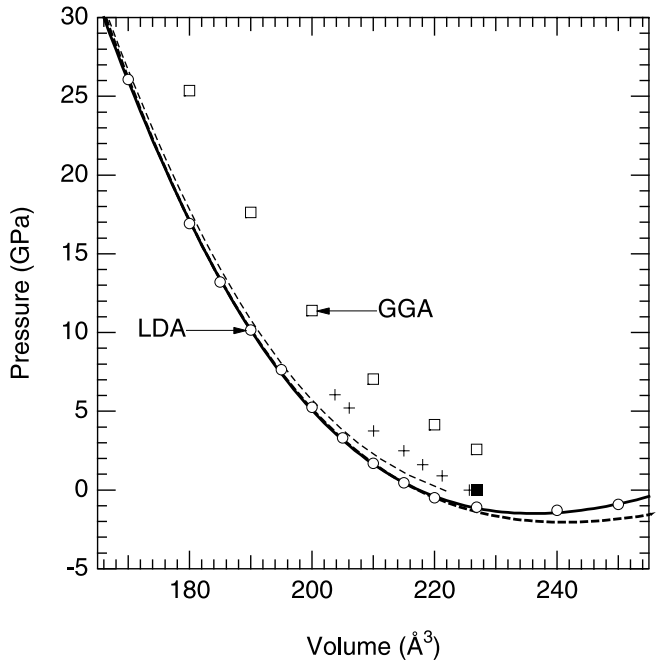

Figure 1. Equation of state of talc: open circles, LDA theory; open squares, GGA theory; solid line, finite strain fit to all LDA results; dashed line, finite strain fit to LDA results for $V < 230$ Å^3; solid square, experimental from *Perdikatsis and Burzlaff* [1981]; crosses, experimental from *Pawley et al.* [1995].

3. Results

[12] The equation of state curve calculated within the local density approximation under static conditions is 5% smaller in volume than that experimentally observed at room temperature (Figure 1 and Table 1). After accounting approximately for thermal effects according to equation (8), the difference in volume between theory and experiment is reduced to 2%. This remaining discrepancy is attributed to the LDA. By comparison, the equation of state calculated within the GGA disagrees substantially with experimental measurement. The

Table 1. Equation of State Parameters of Talc[a]

	Experiment	LDA Static	LDA 300 K	GGA Static
V_0, Å^3	226.9 (1)	217.5 (1)	221.8 (2)	238 (1)
K_0, GPa	41.6 (9)	37.8 (4)	29 (5)	
K_0'	6.5 (4)	13.6 (2)	17	
K_0K_0''	–	−153 (6)	−250	

[a] Numbers in parentheses represent uncertainties in the last digit. Experimental values are from V_0 [*Perdikatsis and Burzlaff*, 1981]; K_0, and K_0' [*Pawley et al.*, 1995]. LDA 300 K values are calculated assuming $\gamma = 0.38 \pm 0.1$, $\theta_D = \theta(1) = 830$ K, $q = 1$.

static GGA equation of state overestimates the volume by 9%. Accounting for thermal corrections increases the magnitude of the discrepancy. Subsequent discussions refer only to LDA results unless otherwise noted.

[13] Our results show that the Eulerian finite strain formulation expanded to fourth order provides an adequate description of talc over a wide range of expansive and compressive strains. In contrast, the universal equation of state is not sufficiently flexible to adequately represent our results, even if only those under compression are considered (Figures 2 and 3). All fits were performed assuming a zero pressure volume $V_0 = 217.5$ Å^3, a value that is tightly constrained by first principles results at small positive and negative static pressures.

[14] The bulk modulus is smaller than that measured experimentally. The effect of thermal pressure is to lower the theoretical value of the bulk modulus further, increasing the magnitude of the discrepancy. This issue is discussed below.

[15] The theoretical equation of state exhibits a spinodal instability [*Born and Huang*, 1954] at a volume $V_{sp} = 236$ Å^3, corresponding to 4% expansion relative to the ambient state as measured experimentally (Figure 1). The spinodal is

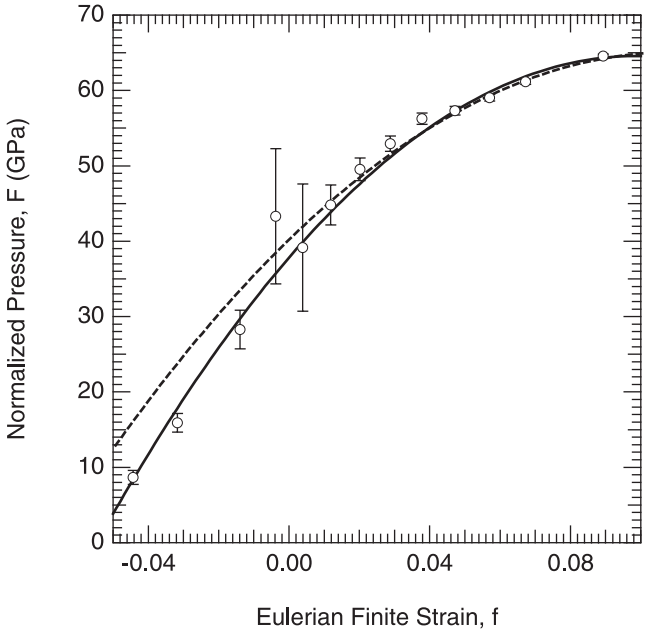

Figure 2. Eulerian finite strain fit to the equation of state of talc: circles, LDA results; error bars calculated on the basis of an assumed numerical precision in the pressure of ±0.1 GPa; solid line, fit to all LDA results; dashed line, fit to LDA results for $V < 230$ Å^3.

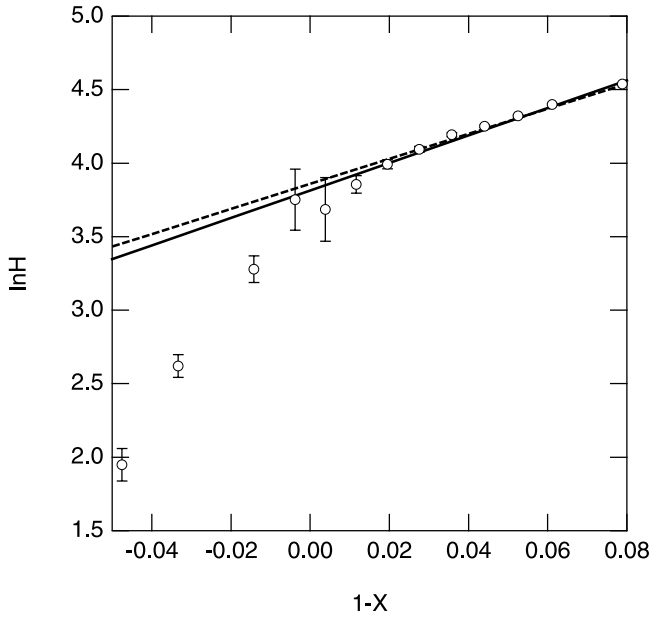

Figure 3. Universal equation of state fit: circles, LDA results; solid line, fit to all LDA results; dashed line, fit to LDA results for $V < 230$ Å^3.

the point at which the bulk modulus vanishes and occurs at that point where the pressure reaches a minimum value. At volumes larger than V_{sp}, the pressure increases with increasing volume, corresponding to a negative bulk modulus.

[16] The compression of talc is highly anisotropic: the *c* axis is 7 times more compressible than the *b* axis; the *a* axis is approximately 30% more compressible than the *b* axis (Figure 4 and Table 2). The axis lengths are plotted as a function of volume rather than as a function of pressure. The reason is that *a* and *b* are not single-valued functions of pressure over the range considered. For volumes larger than V_{sp}, *a* and *b* shrink slightly upon volume expansion, whereas *c* continues to expand. When compared at constant volume, theoretical and experimental determinations of the axis lengths agree to within 1% (Table 3). Values of the angular lattice parameters also agree well with experimental measurements at ambient conditions: to within 0.5° (Figure 5). Theory predicts that β increases upon compression in agreement with the initial trend found by *Pawley et al.* [1995]. The experimental study found that β begins to decrease with increasing pressure at higher compressions, behavior that is not seen in the theoretical results. We find that talc maintains pseudomonoclinic symmetry over the pressure range investigated: α and γ differ significantly from the ideal value of 90°, but by not more than 0.6°. The high-pressure study of *Pawley et al.* [1995] assumed monoclinic symmetry with $\alpha = \gamma = 90°$.

[17] Visual inspection of the predicted structures shows that compression produces significant changes in the size, shape, and orientation of the coordination polyhedra (Figures 6 and 7 and Tables 3 and 4). The SiO_4 tetrahedra and MgO_6 octahedra both decrease in volume with increasing pressure; the polyhedral bulk moduli are $K_{Mg} = 140$ GPa and $K_{Si} = 600$ GPa, respectively. At low pressure, the tetrahedra are more regular than the octahedra. However, the tetrahedra are found to become more distorted upon

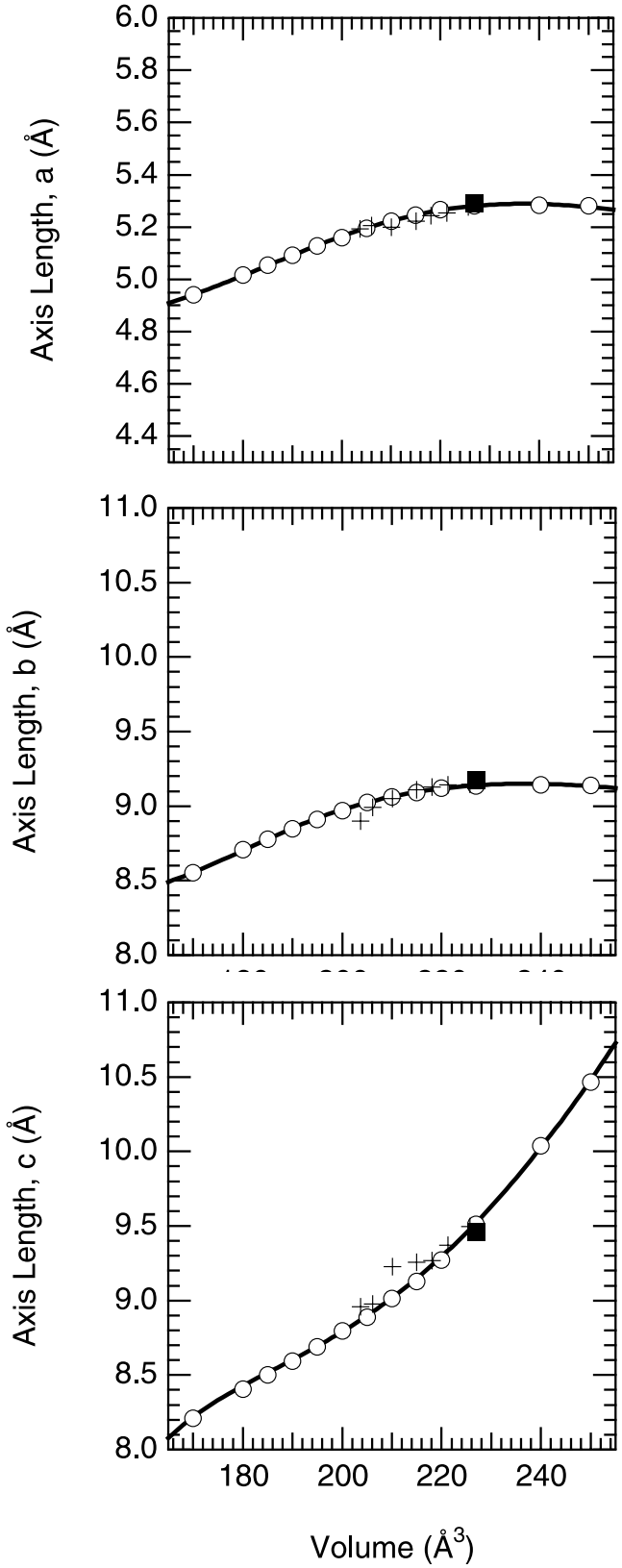

Figure 4. Axis lengths: open circles, LDA results; solid line, fit to LDA results; solid square, experiment from *Perdikatsis and Burzlaff* [1981]; crosses, experiment from *Pawley et al.* [1995].

Table 2. Linear Moduli[a]

	K_a	K_b	$K_{c^{ast}}$
Talc (LDA)	250	350	50
Brucite (reference 1)	261	261	52
Muscovite (reference 2)	371	321	68

[a] In gigapascals. References: 1, *Xia et al.* [1998]; 2, *Vaughan and Guggenheim* [1986].

compression, while the octahedra become more regular. At the highest pressure of our study, the quadratic elongation, Q [*Robinson et al.*, 1971] of tetrahedra and octahedra are nearly identical. The shape of the octahedra may be characterized by the octahedral tilt angle, the angle between the octahedral body-diagonal and the c^* direction [*Bailey*, 1988]

$$\cos\psi = \frac{t}{2\langle r_{\mathrm{Mg-O}}\rangle}, \tag{11}$$

where t is the thickness of the octahedron in the c^* direction and $\langle r_{Mg\text{-}O}\rangle$ is the average Mg-O bond length. At low pressure, we find that the octahedra are slightly flattened in the c^* direction in excellent agreement with experiment: *Perdikatsis and Burzlaff* [1981] find $\psi = 58.43°$. Our results approach the ideal value: $\cos^{-1}(1/\sqrt{3}) \approx 54.7°$ with increasing pressure.

Table 3. Structure of Talc at Selected Values of the Unit Cell Volume[ab].

	Experiment	$V = 226.89$ Å^3	200 Å^3	170 Å^3
a, Å	5.290	5.2812	5.1598	4.9411
b, Å	9.173	9.1369	8.9711	8.5526
c, Å	9.460	9.5111	8.7979	8.2116
α	90.46	90.53	90.47	89.97
β	98.68	98.59	100.80	101.55
γ	90.09	90.06	90.39	90.02
$Mg2_x$	0.5001	0.5005	0.5014	0.5033
$Mg2_y$	0.8333	0.8331	0.8327	0.8318
$Mg2_z$	0.0000	0.0000	0.0000	0.9974
$Si1_x$	0.2453	0.2442	0.2643	0.2729
$Si1_y$	0.5026	0.5029	0.5032	0.4989
$Si1_z$	0.2909	0.2876	0.3101	0.3273
$Si2_x$	0.2459	0.2444	0.2665	0.2793
$Si2_y$	0.8359	0.8363	0.8374	0.8346
$Si2_z$	0.2911	0.2877	0.3100	0.3270
$O1_x$	0.1991	0.1985	0.2085	0.2145
$O1_y$	0.8344	0.8344	0.8355	0.8342
$O1_z$	0.1176	0.1156	0.1241	0.1305
$O2_x$	0.6970	0.6971	0.7049	0.7095
$O2_y$	0.6674	0.6677	0.6682	0.6674
$O2_z$	0.1126	0.1121	0.1238	0.1354
$O3_x$	0.1980	0.1979	0.2042	0.2088
$O3_y$	0.5012	0.5013	0.5005	0.4982
$O3_z$	0.1176	0.1155	0.1242	0.1308
$O4_x$	0.0199	0.0171	0.0667	0.1026
$O4_y$	0.9287	0.9277	0.9539	0.9777
$O4_z$	0.3481	0.3448	0.3676	0.3801
$O5_x$	0.5202	0.5171	0.5669	0.6042
$O5_y$	0.9109	0.9129	0.8902	0.8598
$O5_z$	0.3494	0.3453	0.3757	0.3920
$O6_x$	0.2429	0.2450	0.2186	0.1722
$O6_y$	0.6699	0.6701	0.6708	0.6678
$O6_z$	0.3484	0.3456	0.3676	0.3794
H_x	0.7190	0.7243	0.7412	0.7487
H_y	0.6690	0.6681	0.6668	0.6673
H_z	0.2030	0.2160	0.2368	0.2565

[a] Mg1 at the origin.
[b] From *Perdikatsis and Burzlaff* [1981].

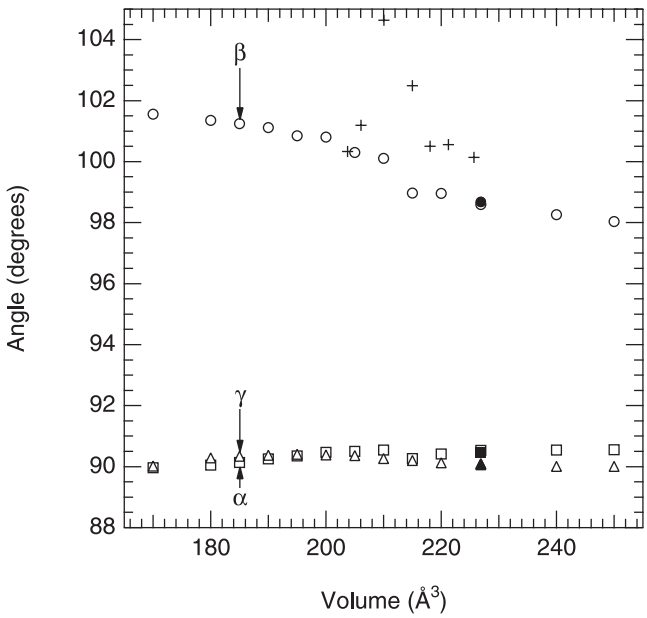

Figure 5. Angular lattice parameters: open symbols, LDA results; solid symbols, experimental values from *Perdikatsis and Burzlaff* [1981]: solid square, α; solid circle, β; solid triangle, γ; crosses, experimental values of β from *Pawley et al.* [1995].

[18] With increasing pressure, significant corrugation develops on the outer edges of the 2:1 sheets: the basal oxygens are significantly noncoplanar at high pressure. Also apparent in representations of the structure is the pressure-induced increase in the tetrahedral rotation angle, defined by

$$\rho = \langle |\theta_{basal} - 120^\circ| \rangle, \tag{12}$$

where θ_{basal} is the angle formed by triples of basal oxygen atoms and the angle brackets indicate the mean value (Figure 8).

[19] Despite large changes in other portions of the structure, the OH bond remains essentially unchanged over the pressure range investigated: the bond remains normal to the $a-b$ plane, and the bond length changes by <0.5%, from 0.977 Å at zero pressure, to 0.973 Å at the highest pressure investigated. For comparison, the value measured by X-ray diffraction at ambient conditions is 0.845 Å [*Perdikatsis and Burzlaff*, 1981].

4. Discussion

4.1. Equation of State and Elasticity

[20] It is widely assumed that the local density approximation leads to overbinding; that is the theoretically calculated volume is smaller than that observed in the laboratory. However, the comparison is often not direct. Whereas most first principles calculations are athermal, most experimental measurements are performed at room temperature. We find that when the effects of temperature and zero-point motion are accounted for, the disagreement between LDA and experiment, while not eliminated, is significantly reduced. Thus, at least in the case of talc, an appropriate account of vibrational contributions is important for evaluating the accuracy of the local density approximation.

[21] In talc, the contribution of zero-point motion to the pressure is substantial and exceeds the contribution due to temperature. The reason is that the characteristic vibrational temperature significantly exceeds 300 K, as is typical of most silicates [*Kieffer*, 1980]. Vibrational contributions to thermodynamics, and zero-point motion in particular, are likely to be important in comparisons of athermal first principles calculations with experimental data at ambient temperature for most silicates [*Kiefer et al.*, 2002].

[22] The local density approximation leads to substantially better agreement with experiment than the generalized gradient approximation. The GGA leads to under-binding in the case of talc; the theoretically predicted athermal volume exceeds that experimentally measured at room temperature. When thermal effects are accounted for, the volume expands, leading to even worse agreement with experiment. It is worth noting in this context some evidence that the

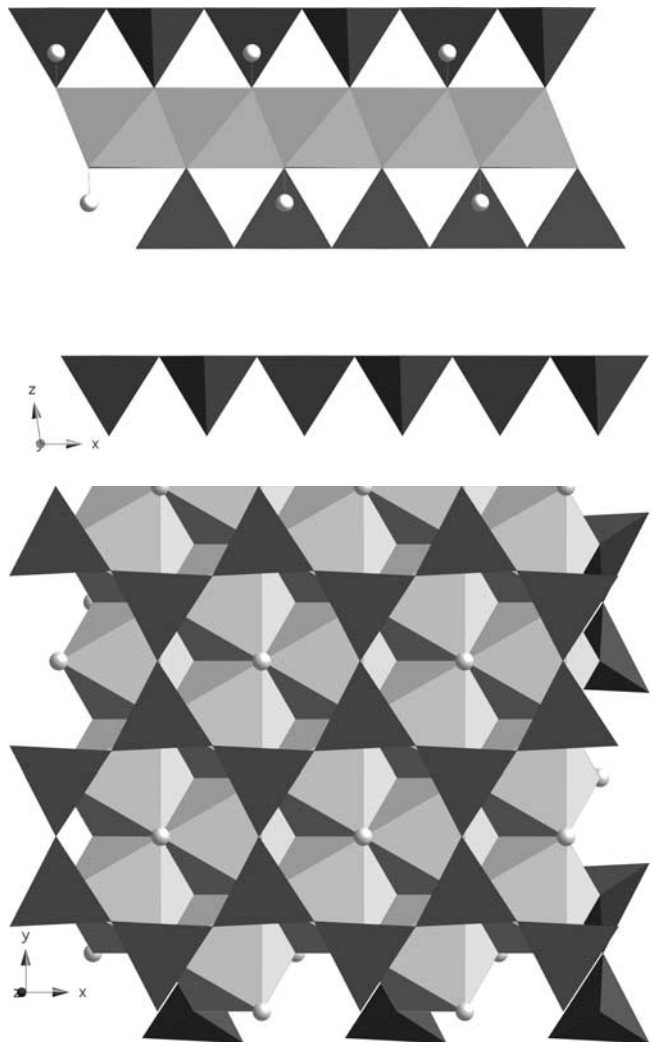

Figure 6. Predicted structure of talc at $V = 226.89$ Å^3 (top) view along b; (bottom) view along c^*. Darker polyhedra, SiO_4 tetrahedra; lighter polyhedra, MgO_6 octahedra; spheres and connecting lines, hydrogens and hydroxyl bonds.

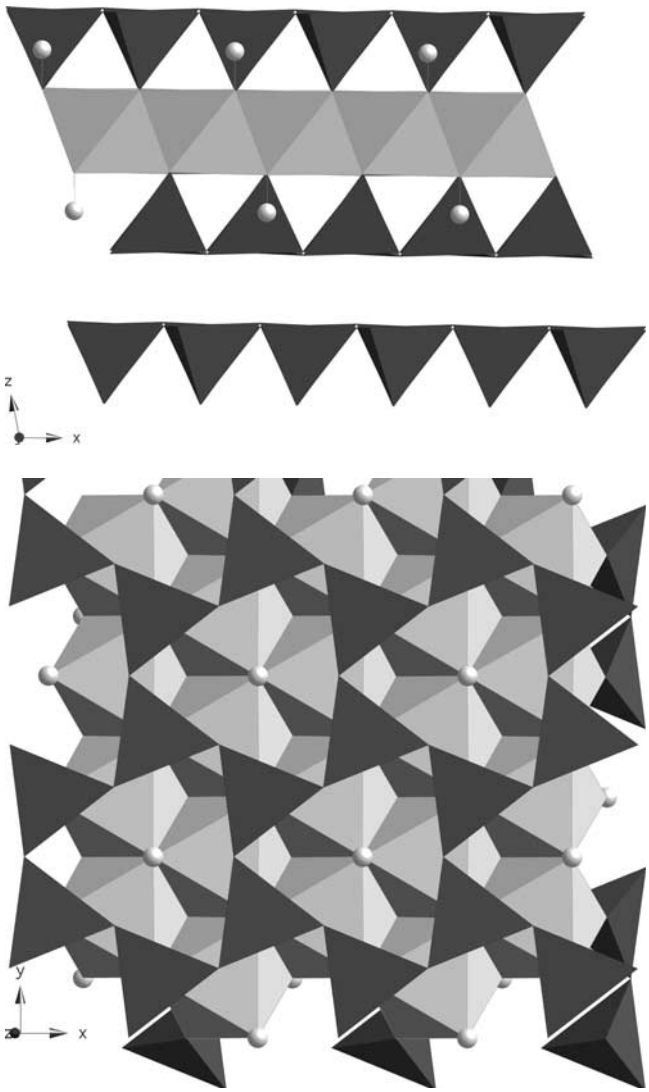

Figure 7. Predicted structure of talc at $V = 170$ Å^3 (top) view along b; (bottom) view along c^*. Symbols as in Figure 6.

GGA yields superior predictions of the relative energetics of silicate phases [*Demuth et al.*, 1999; *Hamann*, 1996].

[23] The differences between theoretical and experimental equations of state, while small, are systematic, as revealed by the discrepancy in the bulk modulus (Table 1). The difference appears to be significant and not due to differences in fitting schemes. For example, if the static theoretical results are fit with a third-order Birch-Murnaghan equation of state, the best fitting value of $K_0 = 36.5$ GPa ($K_0' = 10.3$) is very similar to that obtained from a fourth-order fit. It is unlikely that the discrepancy between theoretical and experimental value of the bulk modulus is due to the LDA, from which one expects an error of the opposite sense. The tendency of LDA to overbind typically leads to an overestimated bulk modulus as well as an underestimated zero pressure volume, in accord with expectations based on modulus-volume systematics [*Anderson and Nafe*, 1965].

Table 4. Properties of Polyhedra at Selected Values of the Unit Cell Volume[a]

Volume, Å^3	P_{static}, GPa	V_{Mg}, Å^3	V_{Si}, Å^3	Q_{Mg}	Q_{Si}	ψ
226.89	−1.10	11.539	2.177	1.0092	1.0000	58.526
220.00	−0.48	11.478	2.175	1.0090	1.0000	58.486
210.00	1.69	11.307	2.165	1.0082	1.0001	58.350
200.00	5.25	11.035	2.153	1.0072	1.0004	58.108
190.00	10.16	10.730	2.138	1.0061	1.0010	57.820
180.00	16.91	10.389	2.119	1.0048	1.0019	57.450
170.00	26.07	10.005	2.097	1.0038	1.0036	57.121

[a] The calculated static pressure is also shown for reference.

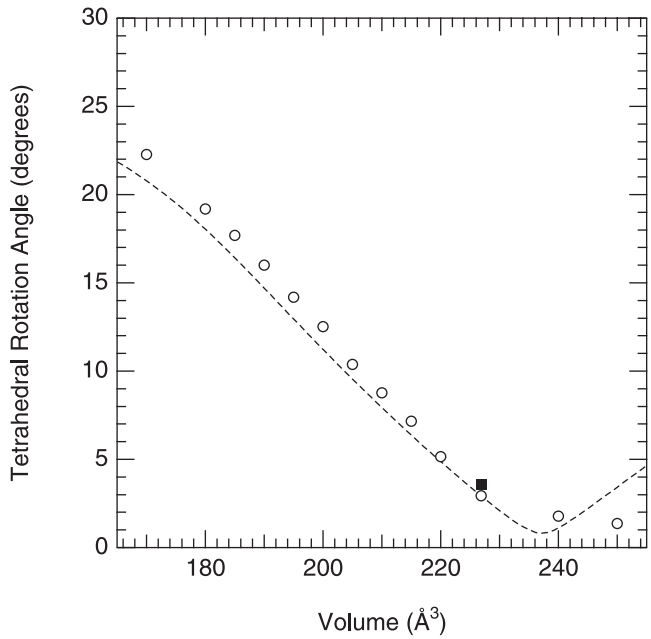

Figure 8. Tetrahedral rotation angle: open circles, LDA results; solid square, experiment from *Perdikatsis and Burzlaff* [1981]; dashed line, calculated from equation (13) using the LDA value of the *b* axis length versus volume and assuming $b_0 = 9.151$ Å.

[24] The effect of lattice vibrations decreases the bulk modulus, thereby increasing the discrepancy between theory and experiment. The vibrational contribution is estimated according to equation (9) for a range of values of the relevant parameters (Figure 9). The calculation depends most strongly on the assumed value of γ. For $\gamma = 0.38$, the bulk modulus at 300 K is 29 GPa, 30% smaller than the theoretical static value. In talc, the effect of vibrations on the bulk modulus is unusually large because of the proximity of the spinodal: as thermal energy is added to the lattice, the system becomes increasingly sensitive to the tensional portion of the equation of state where the bulk modulus decreases rapidly toward zero.

[25] The difference between theoretical and experimental values of the bulk modulus may originate in the distinct elastic response of polycrystals and single crystals. A single crystal is not subject to the requirement of strain compatibility with surrounding crystals and would be expected to obey the Reuss (lower) bound of the elastic moduli, corresponding to conditions of uniform stress. Because the system examined in our theoretical calculations is homogeneous the calculated value of the bulk modulus corresponds to the Reuss bound. In contrast, a polycrystal in which the crystallites are in contact may also be subject to strain compatability and its elastic moduli must therefore be larger

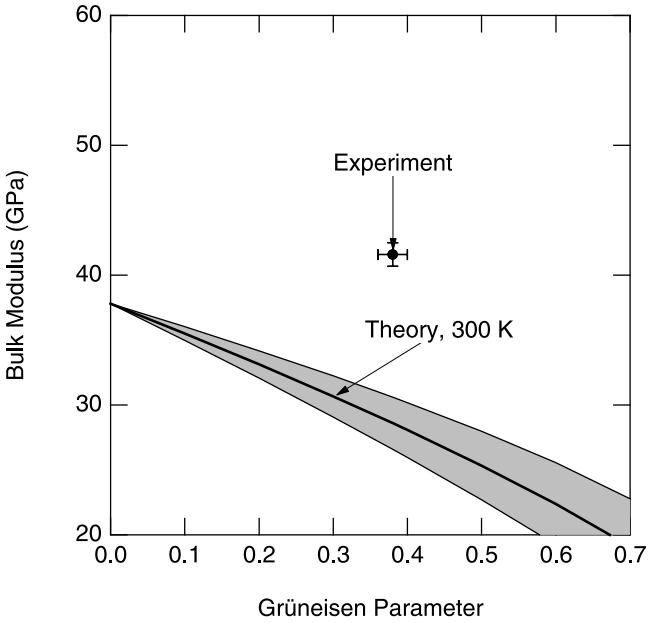

Figure 9. Bulk modulus of talc at 300 K estimated from LDA results and compared with experimental values (symbol) [*Pawley et al.*, 1995]. Shading represents the effects of plausible uncertainties in thermal parameters other than the Grüneisen parameter including θ_D (±100), and q (±0.5).

than the Reuss bound. The difference between the Reuss and Voigt (uniform strain) bounds may be large in the case of highly anisotropic materials such as clays or micas. For example, in muscovite, Reuss and Voigt bounds on the bulk modulus differ by 40% [*Vaughan and Guggenheim*, 1986].

[26] We suggest that because laboratory experiments were performed on a polycrystal, the experimentally measured value of the bulk modulus may be larger than the Reuss bound, and that this may account for the discrepancy between theoretical and experimental values of the bulk modulus. The requirements of strain compatibility may also be responsible for the difference between experimental and theoretical values of K_0'.

4.2. Spinodal

[27] We predict a spinodal instability in talc upon expansion by 4% from the experimental ambient volume. The spinodal is that point where the bulk modulus vanishes, i.e. where pressure is extremal, reaching a minimum value beyond which it decreases no more upon further expansion. At the spinodal, talc is mechanically unstable and would be expected to fragment [*Born and Huang*, 1954]. Thus the pressure of the spinodal, −1.5 GPa, is the theoretical prediction of the hydrostatic tensile strength of talc in defect-free, homogeneous form. This quantity is distinct from the usual tensile strength which is measured under uniaxial tension. Because the talc structure is anisotropic, the uniaxial tensile strength may be substantially less than the hydrostatic tensile strength. The strength measured on a defective crystal, or of a polycrystalline aggregate of talc, may also be substantially less than the strength of perfect single crystal. For comparison, the tensile strength of polycrystalline aggregates of clays (shale) is found to be a few megapascals [*Lockner*, 1995]. Because the spinodal in talc occurs at expansions that are modest, it may be relevant for understanding the thermodynamic properties of talc at high temperature and low pressure, as our estimates of the effect of temperature on the bulk modulus suggest.

4.3. Compression Mechanisms

[28] The compression of many phyllosilicates including talc is highly anisotropic, behavior that is understood in terms of the much weaker bonding between tot layers than within them. Our results confirm these expectations. Predicted structures show that the interlayer distance decreases by 16% upon volume compression by 25%. In contrast, the thickness of the tot sheets measured in the c^* direction changes by only 5% over the same range of volume compression. Compression of the tot sheets is taken up mainly by the tetrahedra: the thickness of the t sheet in the c^* direction shortens by 5.8%, primarily due to shortening of the apical Si-O bond, while that of the o sheet shortens by only 3.3%. We note that a recent study of clinochlore also found that the t sheet was more compressible than the o sheet in the c^* direction; the o sheet was not resolvably thinned over the limited pressure range of the experimental study [*Welch and Marshall*, 2001].

[29] Compression of the a–b plane is taken up primarily by compression of the Mg-octahedra which have a much lower polyhedral bulk modulus than the Si-tetrahedra. This is demonstrated by the similarity of the in-plane compressibility of talc and brucite, a structure that consists of layers of Mg-OH octahedra similar to the o sheet in talc (Table 2). The greater mean in-plane modulus of muscovite may be understood in terms of the stronger Al-O bond of the o sheet in this structure (Table 2).

[30] The polyhedral bulk modulus of the Mg-octahedra in talc is similar to that found for the same polyhedron in other silicates [*Hazen and Finger*, 1979; *Kiefer et al.*, 1999, 2002]. The bulk modulus of the tetrahedra is much larger than that found in other silicates. The reason is that the tetrahedra need not compress in order for the t sheets to maintain registry with the o sheets. Instead, the t sheets respond to in-plane compression by tetrahedral rotation. One can show that the relationship between the b axis length and the tetrahedral rotation angle for ideal tetrahedra is [*Bailey*, 1988]

$$\cos\rho = b/b_0, \tag{13}$$

where b_0 is the ideal value of b, corresponding to no tetrahedral rotation. Our theoretical results follow this relationship closely in the compressional regime: as the b axis shrinks on compression, the tetrahedral rotation angle increases (Figure 8). The relationship is not obeyed in the tensional regime: as the b axis shrinks slightly upon expansion, the tetrahedral rotation angle continues to decrease toward zero.

[31] Since in-plane compression of the tot sheets is governed by the Mg-octahedra, we might expect a relationship between the linear compressibilities of a and b axes and the volume compressibility of the Mg-octahedra. If the Mg-octahedra compress approximately isotropically, the polyhedral bulk modulus should be approximately one third K_a or K_b, the factor of 3 coming from the difference between volume and linear compressibilities. The theoretical results

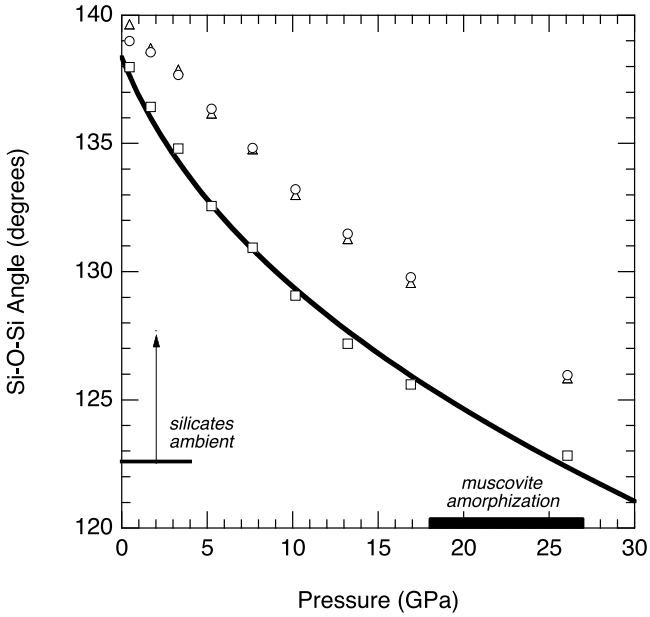

Figure 10. LDA prediction of the Si-O-Si angles in talc (symbols and solid line fit to the variation of the smallest Si-O-Si angle) compared with values observed in silicates at ambient conditions (horizontal line and arrow) [*O'Keeffe and Hyde*, 1978]; and range in pressure over which muscovite is observed to become amorphous (bar) [*Faust and Knittle*, 1994].

do not support this picture. Instead, we find that the a and b axes are significantly softer

$$K_{Mg} = 140 \text{ GPa} > K_b/3 = 120 \text{ GPa} > K_a/3 = 80 \text{ GPa} \quad (14)$$

The octahedral tilt angle shows that at ambient pressure, the octahedra are flattened in the c^* direction, but become more ideal upon compression. In order for this change of shape to occur, the Mg-octahedra must compress more in the a direction and less in the c^* direction. The greater in-plane compressibility of the octahedra explains the difference between the polyhedral bulk modulus, and K_a and K_b. This analysis also explains the relative magnitudes of K_a and K_b: K_a is less than K_b because octahedral tilting, and the pressure-induced change in the tilt angle with pressure, is in the $a-c$ plane.

4.4. High-Pressure Metastability

[32] Talc is thermodynamcally stable to a maximum pressure of 5 GPa where it breaks down to an assemblage of enstatite, coesite, and 10 Å phase [*Chinnery et al.*, 1999]. However, experiments [*Pawley et al.*, 1995] have shown that it is preserved metastably upon compression at room temperature to at least 6 GPa. Similar behavior is seen in many silicates. Materials such as muscovite, quartz, and coesite survive metastably at room temperature to pressures that are many times that of their maximum thermodynamic stability [*Faust and Knittle*, 1994; *Hemley et al.*, 1988]. When the limit of metastability is reached, these materials typically amorphize instead of transforming to the equilibrium phase.

[33] The limit of talc metastability has not yet been characterized in the laboratory. Our theoretical calculations also do not show any amorphization or other transformations up to the maximum pressure studied. However, it is important to recognize that within the framework of our calculations, we do not expect to find an amorphization transition. The contents of the unit cell and the space group symmetry are preserved so that pressure-induced phase transformations occur only if the two phases involved in the transition possess a supergroup-subgroup relationship and have commensurate unit cells.

[34] We suggest that talc may undergo a metastable transformation, possibly to an amorphous state, at a pressure near 25 GPa (Figure 10). This is the pressure at which the smallest Si-O-Si angle in talc falls below 122°, the smallest value found in silicates at ambient conditions. Our estimate of the maximum pressure of talc metastability is consistent with experimental observations of muscovite. This mineral, also a phyllosilicate, becomes gradually amorphous over the pressure range 18–27 GPa.

5. Conclusions

[35] Phyllosilicates, such as talc, provide a stringent test of density functional theory because of the large contrast in the energetics of in-plane versus across-plane compression. Excellent agreement between the experimentally observed structure and equation of state show that the local density approximation captures much of the relevant physics of talc.

[36] Theory allows us to explore portions of the equation of state that are difficult to access experimentally, including the expanded portion where a spinodal instability is found. The Birch-Murnaghan finite strain theory is found to provide an adequate description of talc.

[37] Our results show that the compression of talc is highly anisotropic and that Voigt and Reuss bounds on the bulk modulus of talc may differ substantially. This means that some care is required when analyzing seismic observations in terms of talc-bearing assemblages [e.g., *Bailey and Holloway*, 2000]. The properties of such assemblages may depend strongly on the polycrystalline texture for two reasons: (1) the anisotropy of talc means that seismic wave speeds may depend substantially on the direction of propagation and polarization and (2) the isotropically averaged elastic moduli may in principle fall anywhere within the Voigt and Reuss bounds (or within the somewhat narrower Hashin-Shtrikman bounds) depending on the details of grain shape, size, and orientation.

[38] Our calculations permit a fundamental understanding of the elastic anisotropy of talc in terms of structural compression mechanisms. These show several significant features including the validation of the relationship between the tetrahedral rotation angle and size of the b axis length over a wide compression range, and the important role of decreasing distortion of the Mg-octahedra with increasing pressure in accounting for the magnitude of the in-plane compressibility.

[39] On the basis of the evolution of the Si-O-Si angle, we predict that talc may become amorphous upon metastable compression at room temperature near a pressure of 25 GPa.

[40] **Acknowledgments.** This work supported by the National Science Foundation under grant EAR-9973139.

References

Ahrens, T. J., (Ed.), *A Handbook of Physical Constants: Mineral Physics and Crystallography*, *AGU Ref. Shelf Ser.*, vol. 2, AGU, Washington, D. C., 1995.

Aidun, J., and M. S. T. Bukowinski, Equation of state and metallization of CsI, *Phys. Rev. B*, *29*, 2611–2621, 1984.

Anderson, O. L., *Equations of State of Solids for Geophysics and Ceramic Science*, Oxford Univ. Press, New York, 1995.

Anderson, O. L., and J. E. Nafe, Bulk modulus-volume relationship for oxide compounds and related geophysical problems, *J. Geophys. Res.*, *70*, 3951–3960, 1965.

Bailey, E., and J. R. Holloway, Experimental determination of elastic properties of talc to 800°C, 0.5 GPa: Calculations of the effect on hydrated peridotite, and implications for cold subduction zones, *Earth Planet. Sci. Lett.*, *183*, 487–498, 2000.

Bailey, S. W., Introduction, *Hydrous Phyllosilicates (Exclusive of Micas)*, *Rev. Mineral.*, vol. 19, edited by S. W. Bailey, pp. 1–8, Mineral. Soc. of Am., Washington, D. C., 1988.

Barron, T. H. K., and G. K. White, *Heat Capacity and Thermal Expansion at Low Temperatures*, Kluwer Acad., Norwell, Mass., 1999.

Birch, F., Finite strain isotherm and velocities for single-crystal and polycrystalline NaCl at high-pressure and 300°K, *J. Geophys. Res.*, *83*, 1257–1268, 1978.

Born, M., and K. Huang, *Dynamical Theory of Crystal Lattices*, Oxford Univ. Press, New York, 1954.

Bridgeman, C. H., A. D. Buckingham, N. T. Skipper, and M. C. Payne, Ab-initio total energy study of uncharged 2:1 clays and their interaction with water, *Mol. Phys.*, *89*, 879–888, 1996.

Cannat, M., Emplacement of mantle rocks in the seafloor at mid-ocean ridges, *J. Geophys. Res.*, *98*, 4163–4172, 1993.

Chinnery, N. J., A. R. Pawley, and S. M. Clark, In situ observation of the formation of 10 angstrom phase from talc plus H_2O at mantle pressures and temperatures, *Science*, *286*, 940–942, 1999.

Demuth, T., Y. Jeanvoine, J. Hafner, and J. G. Angyan, Polymorphism in silica studied in the local density and generalized gradient approximations, *J. Phys. Condens. Matter*, *11*, 3833–3874, 1999.

Evans, B. W., and S. Guggenheim, Talc, pyrophyllite, and related minerals, in *Hydrous Phyllosilicates (Exclusive of Micas)*, *Rev. Mineral.*, vol. 19, edited by S. W. Bailey, pp. 225–294, Mineral. Soc. of Am., Washington, D. C., 1988.

Faust, J., and E. Knittle, The equation of state, amorphization, and high-pressure phase-diagram of muscovite, *J. Geophys. Res.*, *99*, 19,785–19,792, 1994.

Fumagalli, P., L. Stixrude, S. Poli, and D. Snyder, The 10 angstrom phase: A high-pressure expandable sheet silicate stable during subduction of hydrated lithosphere, *Earth Planet. Sci. Lett.*, *186*, 125–141, 2001.

Hamann, D. R., Generalized gradient theory for silica phase transitions, *Phys. Rev. Lett.*, *76*, 660–663, 1996.

Hazen, R. M., and L. W. Finger, Bulk modulus-volume relationship for cation-anion polyhedra, *J. Geophys. Res.*, *84*, 6723–6728, 1979.

Heine, V., The pseudopotential concept, *Solid State Phys*, *24*, 1–37, 1970.

Hemley, R. J., A. P. Jephcoat, H. K. Mao, L. C. Ming, and M. H. Manghnani, Pressure-induced amorphization of crystalline silica, *Nature*, *334*, 52–54, 1988.

Hohenberg, P., and W. Kohn, Inhomogeneous electron gas, *Phys. Rev. B*, *136*, 864–871, 1964.

Ita, J. J., and L. Stixrude, Petrology, elasticity, and composition of the mantle transition zone, *J. Geophys. Res.*, *97*, 6849–6866, 1992.

Kiefer, B., L. Stixrude, and R. M. Wentzcovitch, Normal and inverse ringwoodite at high pressures, *Am. Mineral.*, *84*, 288–293, 1999.

Kiefer, B., L. Stixrude, J. Hafner, and G. Kresse, Structure and elasticity of wadsleyite at high pressures, *Am. Mineral.*, *86*, 1387–1395, 2002.

Kieffer, S. W., Thermodynamics and lattice-vibrations of minerals, 4, Application to chain and sheet silicates and orthosilicates, *Rev. Geophys.*, *18*, 862–886, 1980.

Kohn, W., and L. J. Sham, Self-consistent equations including exchange and correlation effects, *Phys. Rev. A*, *140*, 1133–1138, 1965.

Kresse, G., and J. Furthmüller, Efficiency of ab-initio total energy calculations for metals and semiconductors, *Comput. Mater. Sci.*, *6*, 15–50, 1996a.

Kresse, G., and J. Furthmüller, Efficient iterative schemes for ab initio total-energy calculations using a plane-wave basis set, *Phys. Rev. B*, *54*, 11,169–11,186, 1996b.

Kresse, G., and J. Hafner, Ab initio molecular-dynamics for liquid-metals, *Phys. Rev. B*, *47*, 558–561, 1993.

Kresse, G., J. Hafner, and R. J. Needs, Optimized norm-conserving pseudopotentials, *J. Phys. Condens. Matter*, *4*, 7451–7468, 1992.

Lockner, D. A., Rock failure, in *Rock Physics and Phase Relations: A Handbook of Physical Constants*, *AGU Ref. Shelf*, vol. 3, edited by T. J. Ahrens, pp. 127–147, AGU, Washington, D. C., 1995.

Lundqvist, S., and N. H. March, *Theory of the Inhomogeneous Electron Gas*, Plenum, New York, 1987.

Mishima, O., L. D. Calvert, and E. Whalley, Melting ice-I at 77 k and 10 kbar—A new method of making amorphous solids, *Nature*, *310*, 393–395, 1984.

Monkhurst, H. J., and J. D. Pack, Special points for brillouin-zone integrations, *Phys. Rev. B*, *13*, 5188–5192, 1976.

Mysen, B. O., P. Ulmer, J. Konzett, and M. W. Schmidt, The upper mantle near convergent plate boundaries, in *Ultrahigh-Pressure Mineralogy*, *Rev. Mineral.*, vol. 37, edited by R. Hemley and H. K. Mao, pp. 97–138, Mineral. Soc. of Am., Washingtion, D. C., 1998.

Nye, J. F., *Physical Properties of Crystals: Their Representation by Tensors and Matrices*, 2nd ed., Oxford Univ. Press, New York, 1985.

O'Keeffe, M., and B. G. Hyde, On Si-O-Si configurations in silicates, *Acta Crystallogr., Sect. B*, *34*, 27–32, 1978.

Pawley, A. R., S. A. T. Redfern, and B. J. Wood, Thermal expansivities and compressibilities of hydrous phases in the system MgO-SiO_2-H_2O: Talc, phase a and 10-angstrom phase, *Contrib. Mineral. Petrol.*, *122*, 301–307, 1995.

Payne, M. C., M. P. Teter, D. C. Allan, T. A. Arias, and J. D. Joanopoulos, Iterative minimization techniques for ab initio total-energy calculations: Molecular dynamics and confugate gradients, *Rev. Mod. Phys.*, *64*, 1045–1097, 1992.

Perdew, J. P., K. Burke, and M. Ernzerhof, Generalized gradient approximation made simple, *Phys. Rev. Lett.*, *77*, 3865–3868, 1996.

Perdikatsis, B., and H. Burzlaff, Structural refinement of talc $Mg_3[(OH)_2Si_4O_{10}]$, *Z. Kristallogr.*, *156*, 177–186, 1981.

Richet, P., and P. Gillet, Pressure-induced amorphization of minerals: A review, *Eur. J. Mineral.*, *9*, 907–933, 1997.

Robinson, K., G. V. Gibbs, and P. H. Ribbe, Quadratic elongation-quantiative measure of distortion of coordination polyhedra, *Science*, *172*, 567–569, 1971.

Stixrude, L., and M. S. T. Bukowinski, Simple covalent potential models of tetrahedral SiO_2: Applications to α-quartz and coesite at pressure, *Phys. Chem. Miner.*, *16*, 199–206, 1988.

Stixrude, L., R. E. Cohen, and R. J. Hemley, Theory of minerals at high pressure, in *Ultrahigh-Pressure Mineralogy*, *Rev. Mineral.*, vol. 37, edited by R. Hemley and H. K. Mao, pp. 639–671, Mineral. Soc. of Am., Washingtion, D. C., 1998.

Trommsdorff, V., V. L. Sanches-Vizcaino, M. T. Gomez-Pugnaire, and O. Müntener, High pressure breakdown of antigorite to spinifex-textured olivine and orthopyroxene, SE Spain, *Contrib. Mineral. Petrol.*, *132*, 139–148, 1998.

Vanderbilt, D., Soft self-consistent pseudopotentials in a generalized eigenvalue formalism, *Phys. Rev. B*, *41*, 7892–7895, 1990.

Vaughan, M. T., and S. Guggenheim, Elasticity of muscovite and its relationship to crystal struture, *J. Geophys. Res.*, *91*, 4657–4664, 1986.

Vinet, P., J. Ferrante, J. H. Rose, and J. R. Smith, Compressibility of solids, *J. Geophys. Res.*, *92*, 9319–9325, 1987.

Welch, M. D., and W. G. Marshall, High-pressure behavior of clinochlore, *Am. Mineral.*, *86*, 1380–1386, 2001.

Wentzcovitch, R. M., Invariant molecular dynamics approach to structural phase transitions, *Phys. Rev. B*, *44*, 2358–2361, 1991.

Wentzcovitch, R. M., J. L. Martins, and G. D. Price, Ab initio molecular dynamics with variable cell shape: application to $MgSiO_3$ perovskite, *Phys. Rev. Lett.*, *70*, 3947–3950, 1993.

Xia, X., D. J. Weidner, and H. Zhao, Equation of state of brucite: single-crystal brillouin spectroscopy study and polycrystalline pressure-volume-temperature measurement, *Am. Mineral.*, *83*, 68–74, 1998.

L. Stixrude, Department of Geological Sciences, University of Michigan, 425 E. University Ave., Ann Arbor, MI 48109-1063, USA. (stixrude@umich.edu)